The Journal of Immunology

This information is current as of August 4, 2022.

Live Simian Immunodeficiency Virus Vaccine Correlate of Protection: Local Antibody Production and Concentration on the Path of Virus Entry

Qingsheng Li, Ming Zeng, Lijie Duan, James E. Voss, Anthony J. Smith, Stefan Pambuccian, Liang Shang, Stephen Wietgrefe, Peter J. Southern, Cavan S. Reilly, Pamela J. Skinner, Mary L. Zupancic, John V. Carlis, Michael Piatak, Jr., Diane Waterman, R. Keith Reeves, Katherine Masek-Hammerman, Cynthia A. Derdeyn, Michael D. Alpert, David T. Evans, Heinz Kohler, Sybille Müller, James Robinson, Jeffrey D. Lifson, Dennis R. Burton, R. Paul Johnson and Ashley T. Haase

J Immunol 2014; 193:3113-3125; Prepublished online 18 August 2014;
doi: 10.4049/jimmunol.1400820
http://www.jimmunol.org/content/193/6/3113

Supplementary Material **http://www.jimmunol.org/content/suppl/2014/08/18/jimmunol.1400820.DCSupplemental**

References This article **cites 46 articles**, 20 of which you can access for free at:
http://www.jimmunol.org/content/193/6/3113.full#ref-list-1

Why *The JI*? Submit online.

- **Rapid Reviews! 30 days*** from submission to initial decision
- **No Triage!** Every submission reviewed by practicing scientists
- **Fast Publication!** 4 weeks from acceptance to publication

**average*

Subscription Information about subscribing to *The Journal of Immunology* is online at:
http://jimmunol.org/subscription

Permissions Submit copyright permission requests at:
http://www.aai.org/About/Publications/JI/copyright.html

The Journal of Immunology is published twice each month by
The American Association of Immunologists, Inc.,
1451 Rockville Pike, Suite 650, Rockville, MD 20852
Copyright © 2014 by The American Association of Immunologists, Inc. All rights reserved.
Print ISSN: 0022-1767 Online ISSN: 1550-6606.

Downloaded from http://www.jimmunol.org/ by guest on August 4, 2022

Email Alerts Receive free email-alerts when new articles cite this article. Sign up at:
http://jimmunol.org/alerts

Downloaded from http://www.jimmunol.org/ by guest on August 4, 2022

The Journal of Immunology is published twice each month by
The American Association of Immunologists, Inc.,
1451 Rockville Pike, Suite 650, Rockville, MD 20852
Copyright © 2014 by The American Association of
Immunologists, Inc. All rights reserved.
Print ISSN: 0022-1767 Online ISSN: 1550-6606.

Live Simian Immunodeficiency Virus Vaccine Correlate of Protection: Local Antibody Production and Concentration on the Path of Virus Entry

Qingsheng Li,*[,1,2] Ming Zeng,*[,1,3] Lijie Duan,*[,1] James E. Voss,[†,‡,1] Anthony J. Smith,*[,4] Stefan Pambuccian,[§] Liang Shang,* Stephen Wietgrefe,* Peter J. Southern,* Cavan S. Reilly,[¶] Pamela J. Skinner,[‖] Mary L. Zupancic,* John V. Carlis,[#] Michael Piatak, Jr., Diane Waterman,[††] R. Keith Reeves,[‡‡,§§] Katherine Masek-Hammerman,[‡‡,§§] Cynthia A. Derdeyn,[¶¶] Michael D. Alpert,[‡‡,‖‖] David T. Evans,[‡‡,‖‖,5] Heinz Kohler,[##] Sybille Müller,*** James Robinson,[†††] Jeffrey D. Lifson,** Dennis R. Burton,[†,‡] R. Paul Johnson,[‡,‡‡,6] and Ashley T. Haase***

We sought design principles for a vaccine to prevent HIV transmission to women by identifying correlates of protection conferred by a highly effective live attenuated SIV vaccine in the rhesus macaque animal model. We show that SIVmac239Δnef vaccination recruits plasma cells and induces ectopic lymphoid follicle formation beneath the mucosal epithelium in the rhesus macaque female reproductive tract. The plasma cells and ectopic follicles produce IgG Abs reactive with viral envelope glycoprotein gp41 trimers, and these Abs are concentrated on the path of virus entry by the neonatal FcR in cervical reserve epithelium and in vaginal epithelium. This local Ab production and delivery system correlated spatially and temporally with the maturation of local protection against high-dose pathogenic SIV vaginal challenge. Thus, designing vaccines to elicit production and concentration of Abs at mucosal frontlines could aid in the development of an effective vaccine to protect women against HIV-1. ***The Journal of Immunology*****, 2014, 193: 3113–3125.**

Although there have been substantial and continuing advances in preventing HIV-1 infection, an effective HIV-1 vaccine is still critically needed, particularly to prevent transmission to the young women who bear the brunt of infection in the pandemic's epicenter in Africa (1, 2). To that end, we have been seeking design principles to guide HIV-1 vaccine development by identifying correlates of the robust protection afforded by the live attenuated SIV_{mac239}Δnef vaccine (3–7) against high-dose vaginal challenge in the SIV rhesus macaque (RM) model of HIV-1 transmission to women.

To identify correlates of protection in this animal model in vivo within the female reproductive tract (FRT) tissues, we investigated the very early stages of infection and the maturation of SIV_{mac239}Δnef-associated protection for two reasons. First, exist-

*Department of Microbiology, Medical School, University of Minnesota, Minneapolis, MN 55455; [†]Department of Immunology and Microbial Science, International AIDS Vaccine Initiative Neutralizing Antibody Center, and Center for HIV/AIDS Vaccine Immunology and Immunogen Design, The Scripps Research Institute, La Jolla, CA 92037; [‡]Ragon Institute of MGH, MIT, and Harvard, Charlestown, MA 02129; [§]Department of Laboratory Medicine and Pathology, Medical School, University of Minnesota, Minneapolis, MN 55455; [¶]Division of Biostatistics, School of Public Health, University of Minnesota, Minneapolis, MN 55455; [‖]Department of Veterinary and Biomedical Sciences, College of Veterinary Medicine, University of Minnesota, St. Paul, MN 55108; [#]Department of Computer Science and Engineering, College of Science and Engineering, University of Minnesota, Minneapolis, MN 55455; **AIDS and Cancer Virus Program, Science Applications International Corporation–Frederick, Inc., National Cancer Institute, Frederick, MD 21702; [††]ZeptoMetrix Corporation, Buffalo, NY 14202; [‡‡]New England Primate Research Center, Harvard Medical School, Southborough, MA 01772; [§§]Infectious Disease Unit, Department of Medicine, Massachusetts General Hospital, Boston, MA 02115; [¶¶]Department of Pathology and Laboratory Medicine and Emory Vaccine Center, Emory University, Yerkes, Atlanta, GA 30329; [‖‖]Department of Microbiology and Immunobiology, Harvard Medical School, Boston, MA 02115; [##]Department of Microbiology and Immunology and Molecular Genetics, University of Kentucky, Lexington, KY 40536; ***ImmPheron Inc., Lexington, KY 40509; and [†††]Department of Pediatrics, Center for Infectious Diseases, Tulane University, New Orleans, LA 70112

[1]Q.L., M.Z., L.D., and J.E.V. contributed equally to this work.

[2]Current address: Nebraska Center for Virology, School of Biological Sciences, University of Nebraska, Lincoln, NE.

[3]Current address: Center for Genetics of Host Defense, University of Texas Southwestern Medical School, Dallas, TX.

[4]Current address: Bridge-to-MD Program, American University of Antigua, represented by Manipal Education Americas, LLC.

[5]Current address: AIDS Vaccine Research Laboratory, Pathology and Laboratory Medicine, University of Wisconsin, Madison, WI.

[6]Current address: Yerkes National Primate Research Center, Emory University, Atlanta, GA.

Received for publication March 31, 2014. Accepted for publication July 16, 2014.

This work was supported by a grant from the International AIDS Vaccine Initiative (to A.T.H.); National Institutes of Health Grants AI 086922 (to A.T.H.), AI 071306 and RR00168 (to R.P.J.), AI095985 (to R.P.J. and A.T.H.), and AI 055332 and 1UM1AI100663 (to D.R.B.); a Center for HIV/AIDS Vaccine Immunology/HIV Vaccine Trials Network Early Stage Investigator award and Grant U19 AI 067854 (to R.K.R.); a Ragon Fellowship (to J.E.V.); and by federal funds from the National Cancer Institute, National Institutes of Health under Contract HHSN261200800001E and the National Institutes of Health/National Institute of Allergy and Infectious Diseases Reagent Resource Support Program for AIDS Vaccine Development, Quality Biological, Inc., Gaithersburg, MD (National Institute of Allergy and Infectious Diseases Division of AIDS Contract HHSN272201100023C).

Address correspondence and reprint requests to Dr. Ashley T. Haase, Department of Microbiology, Medical School, University of Minnesota, MMC 196, 420 Delaware Street S.E., Minneapolis, MN 55455-0312. E-mail address: haase001@umn.edu.

The online version of this article contains supplemental material.

Abbreviations used in this article: ADCC, Ab-dependent cell-mediated cytotoxicity; CK5, cytokeratin 5; CVF, cervical vaginal tissues and fluid; FcRn, neonatal FcR; FRT, female reproductive tract; gp41t, trimeric gp41; ISH, in situ hybridization; RIHC, reverse immunohistochemistry; RM, rhesus macaque; SA, staphylococcal protein A; sgp41t, soluble trimeric gp41; TCLA, tissue culture laboratory adapted; TZ, transition zone; VL, viral tissue load; WB, Western blot; WT, wild-type.

Copyright © 2014 by The American Association of Immunologists, Inc. 0022-1767/14/$16.00

www.jimmunol.org/cgi/doi/10.4049/jimmunol.1400820

Downloaded from http://www.jimmunol.org/ by guest on August 4, 2022

ing immune responses or responses that can be deployed rapidly in early infection would be working at favorable odds against the small infected founder populations established at the portal of entry (1). Thus, a correlate of protection might be recognizable as local innate or adaptive immune mechanisms that could inhibit the establishment and expansion of these infected founder populations. Second, $SIV_{mac239}\Delta nef$ vaccination's protective effects mature over time. Animals are not significantly protected if challenged at 5 wk following vaccination, whereas there is sterilizing protection or attenuated infection with challenges at ≥15 wk after vaccination (8). Thus, protection would be expected to correlate with immune responses that increase between 5 wk and later challenge. We show in this study that one striking correlate of the maturation of protection at the portal of entry between 5 and 20 wk postvaccination is a vaccine-induced system to locally produce IgG Abs reactive with the SIV envelope glycoprotein gp41 and to concentrate these Abs on the path of virus entry by the neonatal FcR (FcRn) (9) operating in mucosal epithelium.

Materials and Methods

Animals, vaccination, and vaginal challenge

FRT tissue correlates of protection were analyzed in tissues collected and archived in a cross-sectional serial necropsy study of 19 $SIV_{mac239}\Delta nef$-vaccinated female RM monkeys (*Macaca mulatta*); 8 of the 19 animals were necropsied at 5 and 20 wk postvaccination ($n = 4$ animals/group) to assess the maturation of protection in FRT tissues. The remaining 11 animals were necropsied at 4, 5, 7, or 11 d post–high-dose vaginal challenge at 20 wk postvaccination. The postchallenge archived tissues from the 11 vaccinated animals were compared with FRT tissues from 11 unvaccinated animals that were collected and archived from days 4 to 10 following vaginal challenge (10). Protection also was evaluated in a separate longitudinal study (R.K. Reeves, manuscript in preparation) in which plasma viral tissue loads (VLs) were monitored following vaginal challenge at 5, 20, and 40 wk postvaccination in 18 animals. All of the vaccinated and unvaccinated animals in the cross-sectional studies, as well as animals in the longitudinal study, were vaginally inoculated atraumatically twice on the same day (separated by 4 h) with 10^5 50% tissue culture-infective dose in 1 ml of the same 2004 stock of SIV_{mac251} [supplied by Dr. Christopher Miller, University of California Davis, Davis, CA, and described in Miller et al (10)]. Animals were vaccinated by infecting i.v. with $SIV_{mac239}\Delta nef$ (supplied by Dr. Ronald Desrosiers, Harvard Medical School, Boston, MA). All of the animals were housed in accordance with the regulations of the American Association of Accreditation of Laboratory Animal Care and the standards of the Association for Assessment and Accreditation of Laboratory Animal Care International at the New England and California Primate Centers. Vaccinated animals in the cross-sectional tissue and longitudinal studies were housed under identical conditions at the New England Primate Center.

Tissue collection and processing

At the time of euthanasia, tissues were collected and fixed in 4% paraformaldehyde or SafeFix II and embedded in paraffin for later sectioning and analysis. To examine the endocervical and transition zone (TZ) of endocervix and ectocervix where infected cell founder populations and local expansion were observed in unvaccinated animals (10–12), the uterus, cervix, and vagina were dissected en block. The relevant region of cervix was dissected away from most of the uterus and vagina and then divided into four quadrants. Tissue pieces from each quadrant were snap-frozen and fixed as described or were used unfixed for other assays.

In situ hybridization

In situ hybridization (ISH) with ^{35}S-labeled SIV-specific riboprobes to detect SIV RNA^+ cells was performed, as previously described (11), on 20 sections each of cervix and vagina. In developed radioautographs viewed in reflected light, SIV RNA^+ cells appear green.

Immunohistochemistry and immunofluorescence

Immunohistochemistry and immunofluorescence were performed as previously described (11, 13). Positive stained cells or follicles were enumerated in 20 randomly acquired, high-power images (200× or 400× magnification) by manual counting.

RNA extraction

Frozen cervical specimens were homogenized with a power homogenizer in TRIzol reagent without thawing. Total RNA was isolated, according to the manufacturer's protocol, and further purified with an RNeasy Mini Kit.

Real-time RT-PCR to determine $SIV_{mac239}\Delta nef$ and wild-type SIV_{mac251} viral loads in tissues and plasma

RT-PCR assays were performed, as described, with specific primers to determine the levels of $SIV_{mac239}\Delta nef$ and SIV_{mac251} but with modifications for tissue RNA to accommodate the higher amounts and complexity of input RNA (14).

Isolation of Abs from tissues and cervical vaginal fluids, IgG and IgA determinations, and Western blot analysis

Snap-frozen tissues were homogenized in T-PER tissue protein extraction reagent with 1× Halt Protease Inhibitor, and the protein layer was collected by centrifugation. Cervical vaginal fluids were extracted from Weck-Cel sponges by eluting with 0.25% BSA and 10% IGEPAL (15). IgG and IgA in sera and tissue extracts were measured using ELISA commercial kits (Immunology Consultants Laboratory, Portland, OR). After incubating diluted samples in the ELISA plate, the plates were washed, incubated with anti-human IgG/IgA-HRP, washed again, and developed with tetramethylbenzidine substrate; the absorbance was measured at 450 nm. SIV-specific Abs were detected in Western blot (WB) strips, normalized for total protein in the tissue extracts and sera of individual animals, and developed under conditions that maximized visualization of SIV-specific Ags with the least background. SIV-specific bands were quantified using the Bio-Rad GS-700 densitometer system, expressed as a percentage of the SIV^+ control band assayed concurrently, and normalized for the IgG concentrations of the tissue Abs.

Soluble trimeric gp41

The recombinant gp41 ectodomain (Supplemental Fig. 2) was expressed in 293F cells from a phCMV plasmid that included gp160 residues 554–676 (SIV_{mac239} numbering), which was flanked N-terminally by an IgK signal sequence to target the protein to the endoplasmic reticulum for glycosylation, disulfide bond formation, and secretion and flanked C-terminally by a strep tag for affinity purification from Freestyle 293 media using Strep-Tactin resin. Avidin was added to the filtered media to block biotin before loading onto the column. The column was washed with PBS, and protein was eluted with 2.5 mM desthiobiotin. The eluent was loaded on a Superdex 200 column to purify a 66-kDa protein from higher molecular mass aggregates (~1 mg from 2 l). This size is consistent with a trimeric quaternary structure, likely the six-helix bundle, which was solved previously by X-ray crystallography and nuclear magnetic resonance spectroscopy (16) (*inset*, Supplemental Fig. 2b).

Reverse immunohistochemistry

For reverse immunohistochemistry staining to detect gp41-specific Ab in cells, the heat step for Ag retrieval was omitted to avoid nuclear staining artifacts. After deparaffinization and rehydration, tissue sections were blocked overnight at 4°C with SNIPER Blocking Reagent and then with an Avidin/Biotin Blocking Kit to minimize binding to endogenous biotin. Sections were incubated with Strep-tagII–labeled gp41 Ag, followed by incubation with anti–Strep-tagII mAb conjugated to HRP. Sections were then stained using DAB as substrate, counterstained with Harris hematoxylin, and mounted in Permount. As specificity controls, the Strep-tagII mAb alone did not stain plasma cells or reserve epithelium and, in combination with the Strep-tagII–labeled gp41, it did not stain these cells in FRT tissues from animals not infected with SIV.

Neutralization assays

Protease inhibitors and the nondenaturing detergents in the tissue extracts were removed by ultrafiltration (100 kDa) and replaced by RPMI 1640 containing 10% normal rhesus sera. Tissue extracts and sera were serially diluted (10-fold) in RPMI 1640 containing 10% normal rhesus sera as a source of complement, which was reported to increase neutralization activity in sera from RMs vaccinated with $SIV_{mac239}\Delta nef$ (17). Diluted samples were coincubated with tissue culture laboratory-adapted (TCLA) SIV_{mac251}, $SIV_{mac251\ 32H}$, or SIV_{mac251} vaginal challenge stock at 37°C for 1 h before the addition of C8166-45-SEAP reporter cells (multiplicity of infection = 0.05). The secreted alkaline phosphatase activities were measured after 72 h of incubation (18).

Downloaded from http://www.jimmunol.org/ by guest on August 4, 2022

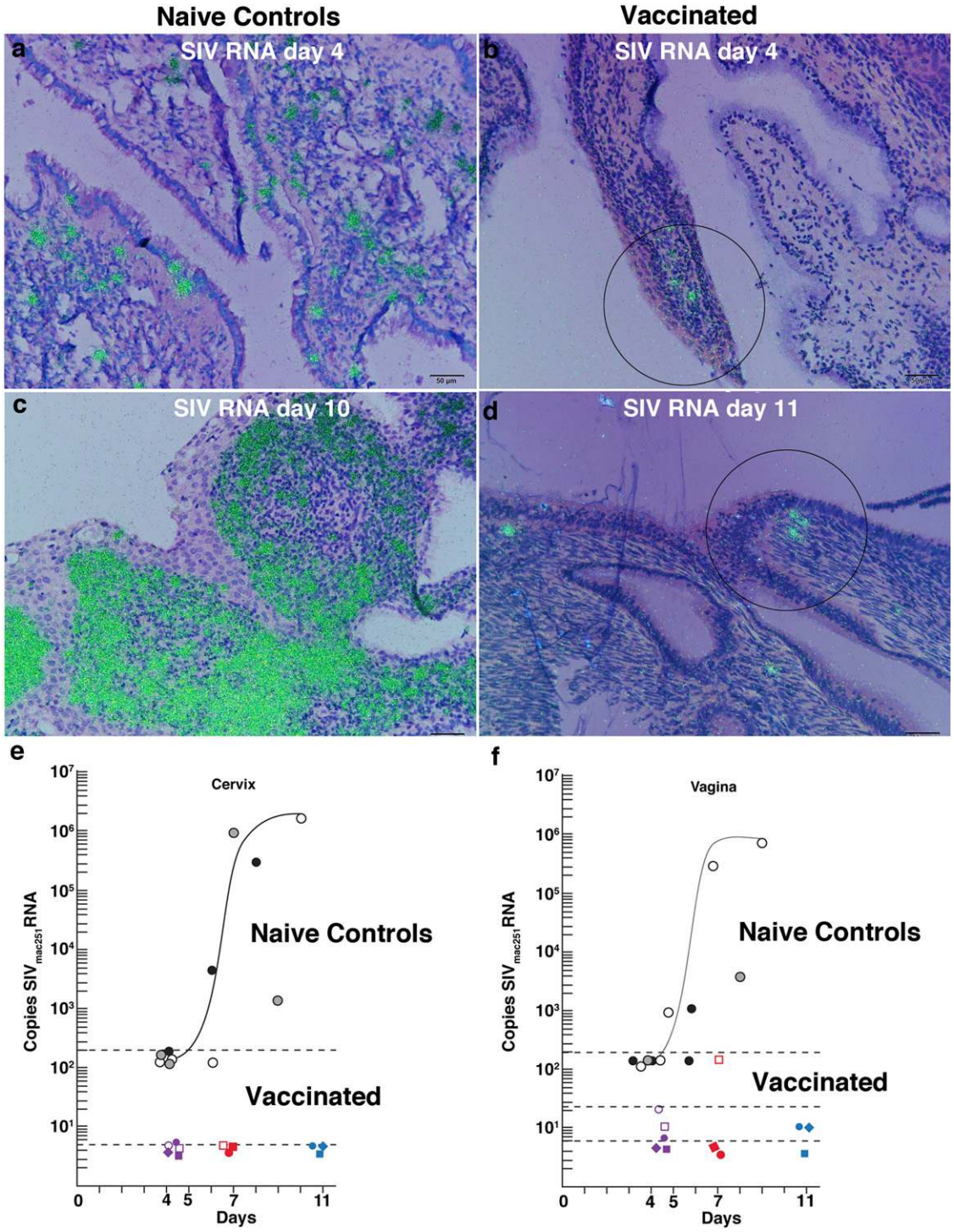

FIGURE 1. Vaccine-associated inhibition of infection in the cervix and vagina. (**a**) Founder population of SIV RNA$^+$ cells (green) detected by ISH (see *Materials and Methods*) in the cervix of an unvaccinated animal 4 d after high-dose vaginal inoculation with SIV_{mac251}. Scale bar, 50 μm. (**b**) Small focus of SIV RNA$^+$ cells (circled) in a vaccinated animal at 4 d after vaginal challenge with SIV, as described in (a). (**c**) Local expansion of SIV RNA$^+$ cells in the cervix, naive control, at day 10, peak viral replication. (**d**) No local expansion in vaccinated animals postvaginal challenge. Three SIV RNA$^+$ cells are circled. (**e** and **f**) Copies of SIV_{mac251}/μg cervical and vaginal tissue RNA plotted against days postvaginal challenge through peak. Filled or unfilled black and gray circles represent individual unvaccinated animal controls (10). Copy numbers for individual vaccinated animals are indicated by colored symbols. The curved line depicts an in vivo growth curve for these tissues in unvaccinated animals. The black dashed lines indicate the limits of detection of the assays at the times they were performed.

In vitro culture model assessment of potential protective mechanisms

The SIV transcytosis assay was modified from Shen et al. (19). A total of 10^6 HEC-1A cells was seeded on 24-Transwell polycarbonate permeable membranes to establish a tight, polarized monolayer of HEC-1-A cells, and monolayers were used only when the transepithelial electrical resistance was ≥700 Ω/cm^2. Ab-mediated blockade of transcytosis was measured in cervical tissue extracts from vaccinated RMs; sera from vaccinated RMs or a chronically infected RM; uninfected RM sera; serum from the chronically infected RM plus staphylococcal protein A (SA) as a competitive inhibitor of FcRn-mediated transport of IgG (20, 21); and the rhesus monoclonal 4.9c Ab that reacted with oligomeric gp41 identically to the Abs in the cervical tissues. Dilutions were added to the basolateral

Downloaded from http://www.jimmunol.org/ by guest on August 4, 2022

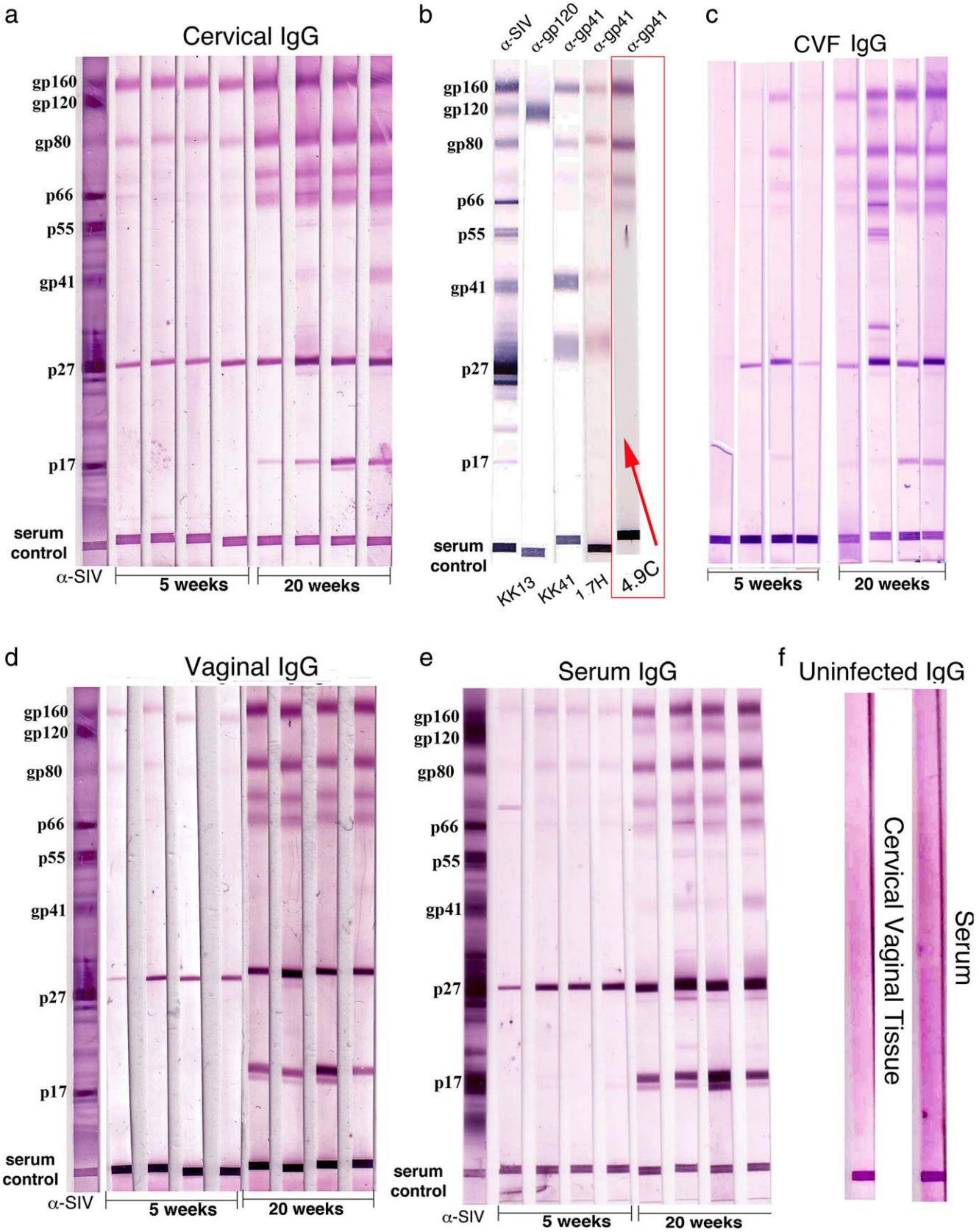

FIGURE 2. Increased SIV-gp41 IgG Abs correlate with the temporal maturation of protection. Each lane in the WBs represents an individual animal. (**a**, **c**, and **d**) Increases, between 5 and 20 wk, in IgG Abs in cervical vaginal tissue extracts or fluids reacting with oligomeric Env gp41 Ags -gp160, gp80, and two other glycoproteins of lower molecular mass. Lanes marked α-SIV indicate positive-control polyclonal Ab; serum control indicates that sample was loaded. (**b**) Rhesus mAbs to gp41 and gp120 identify prominent Env Ag bands as oligomeric gp41. The band at ~31 kDa is thought to be a truncated species of gp41. The WB lane with a rhesus mAb 4.9C, which reacts identically to cervical tissue Abs to oligomeric gp41, is indicated by a red box and arrow. (**e**) Similar increases and SIV reactivities in IgG in serum. (**f**) Cervical vaginal tissue and serum controls in tissues not infected with SIV.

Downloaded from http://www.jimmunol.org/ by guest on August 4, 2022

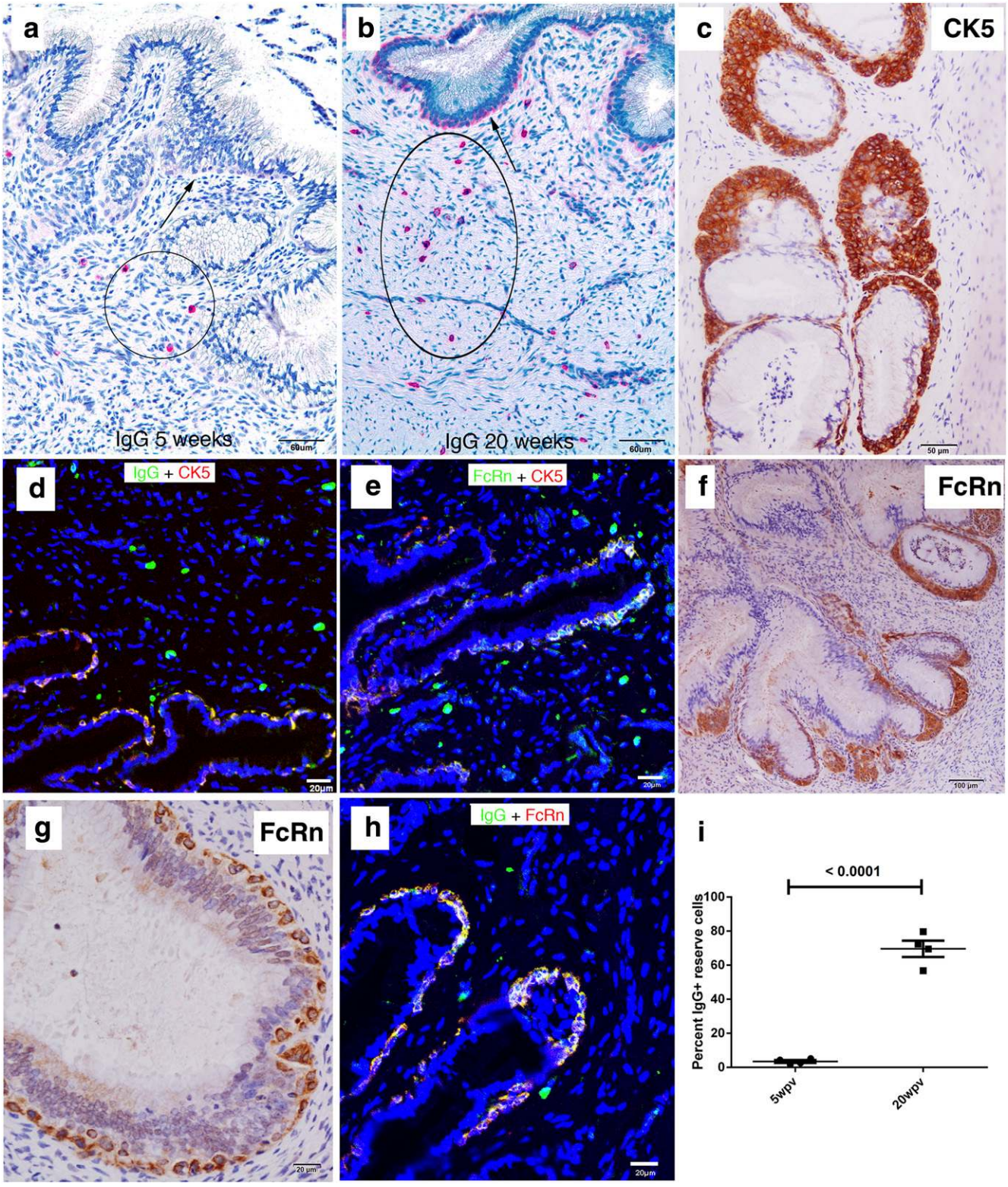

FIGURE 3. Increases between 5 and 20 wk in IgG^+ plasma cells and IgG^+FcRn^+ cervical reserve epithelium. (**a** and **b**) Red-stained IgG^+ cells with plasma cell morphology (circled) in the submucosa at 5 and 20 wk. Scale bars, 60 μm. Arrows point to cells with epithelial morphology aligned beneath the columnar epithelium identified in (**c** and **d**) as $CK5^+$ IgG^+ cervical reserve epithelium. Scale bars, 50 μm (c), 20 μm (d). (**e**) $CK5^+$ cervical reserve epithelium is $FcRn^+$. Scale bar, 20 μm. (**f** and **g**) Brown-stained $FcRn^+$ cells with identical morphology and location beneath the columnar epithelium as $CK5^+$ cervical reserve epithelium shown in (c). Scale bars, 100 μm (f), 20 μm (g). (**h**) IgG is concentrated in the $FcRn^+$ reserve epithelium. Scale bar, 20 μm. (**i**) Quantification of the relative numbers of IgG^+ plasma cells in the submucosa and IgG^+ cervical reserve epithelium at 5 and 20 wk. Four animals were analyzed each at 5 and 20 wk.

and apical compartments of the Transwell and incubated with HEC-1-A cells for 24 h. Thereafter, $SIV_{mac251\ 32H}$ was added to the apical chamber of the Transwell. Transcytosis was assessed after 6 and 24 h by measuring p27 Ag in the basal chamber with a SIV p27 ELISA kit. Inhibition of SIV transcytosis was expressed as the percentage of p27 Ag recovered in the basal chamber in the presence of Abs from different sources compared with the amount of p27 Ag recovered in the presence of uninfected RM serum (defined as 100% transcytosis efficiency). To measure intracellular

Downloaded from http://www.jimmunol.org/ by guest on August 4, 2022

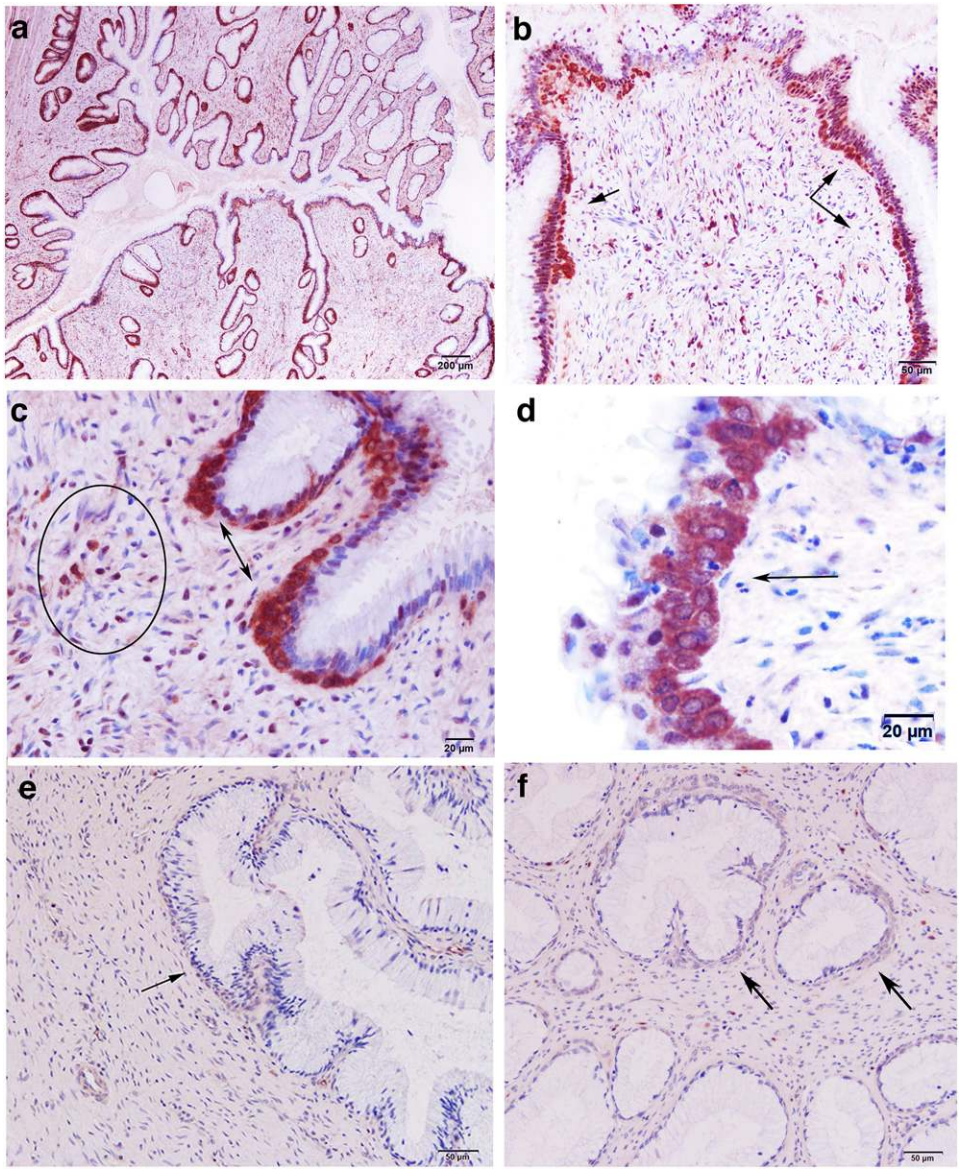

FIGURE 4. Abs reactive with gp41t at 20 wk in cervical reserve epithelium, plasma cells, and ectopic follicles. Sgp41t (Supplemental Fig. 2) with a Strep-tag for detection was used in RIHC to stain cells with Abs reacting with sgp41t. (**a** and **b**) Brown-stained reserve epithelium beneath lining epithelium (arrows). Scale bars, 200 μm (a), 50 μm (b). (**c**) Brown-stained gp41t$^-$ Ab$^+$ reserve epithelium (double-headed arrows) and plasma cells (circled). Scale bar, 20 μm. (**d**) High-power view of stained cervical reserve epithelium (arrow) just below the columnar epithelium lining the cervix. Scale bar, 20 μm. (**e** and **f**) Background staining in two naive controls. Arrows point to cervical reserve epithelium. Scale bars, 50 μm.

SIV p27, HEC-1-A cells were washed extensively with PBS and lysed, and SIV p27 in the intracellular extracts was measured with the SIV p27 ELISA kit. For the analysis of intracellular Ab location, HEC-1-1-A cells on the transmembrane were fixed briefly with SafeFix, permeabilized with 1% Triton X-100, and immunofluorescently stained for IgG and TOTO-3. The transmembranes with the HEC-1-A cells were harvested and mounted on microscope slides using Aqua Poly/Mount. Immunofluorescent micrographs were taken using an Olympus FV1000 FluoView confocal microscope; images were acquired, and mean fluorescence intensity was analyzed using Olympus FluoView software (version 1.7a)

Statistical methods

To test for differences between groups, pairwise two-sample, equal variance *t* tests were conducted after logarithmically transforming the data (because errors for intensity measurements are typically multiplicative) and adding the value 1 to all observations (because some measurements are 0). Differences were deemed significant at $p < 0.05$. All computations were done using statistical software R, version 2.10.1. Figs. 6 and 8 were created in GraphPad Prism. For Fig. 8g, colocalization of pixels was measured with Pearson correlation coefficients, as computed using software for the confocal microscope.

Results

Vaccination effects in the early stages of infection

$SIV_{mac239}\Delta nef$ vaccination was associated with inhibition of the establishment and local expansion of small founder populations of SIV RNA$^+$ cells in the TZ and adjoining endocervix (10–12). In naive unvaccinated controls, SIV RNA$^+$ cells were shown to be detectable as early as 3 or 4 d following high-dose vaginal exposure to wild-type (WT) SIV_{mac251}. These founder populations greatly expand between days 7 and 10–14, at the peak of local replication (Fig. 1a, 1c) (11, 12). In striking contrast, SIV RNA$^+$ cells were detected only rarely in the vaccinated animals at days 4 and 5 postvaginal exposure to high doses of WT SIV_{mac251} at 20 wk postvaccination, and there was no evidence of local expansion (Fig. 1b, 1d). We quantified these differences from exponential expansion to peak replication by PCR determinations of VLs and found that VLs in cervix and vagina were reduced from an average of 5.8×10^5 copies/μg tissue RNA in four unvaccinated animals (10) to undetectable levels in the cervical tissues of 6/6 vaccinated animals and in the vaginal tissues of 3/6 vaccinated animals and an average of 50 copies/μg in 3/6 animals (Fig. 1e, 1f).

IgG Abs to oligomeric gp41 correlate with maturation of protection

We hypothesized that SIV-specific Abs at the portal of entry prior to challenge are at the "right place and time" to account for the rapid inhibition of establishment and expansion of infected founder populations just described; therefore, we looked for prechallenge

Downloaded from http://www.jimmunol.org/ by guest on August 4, 2022

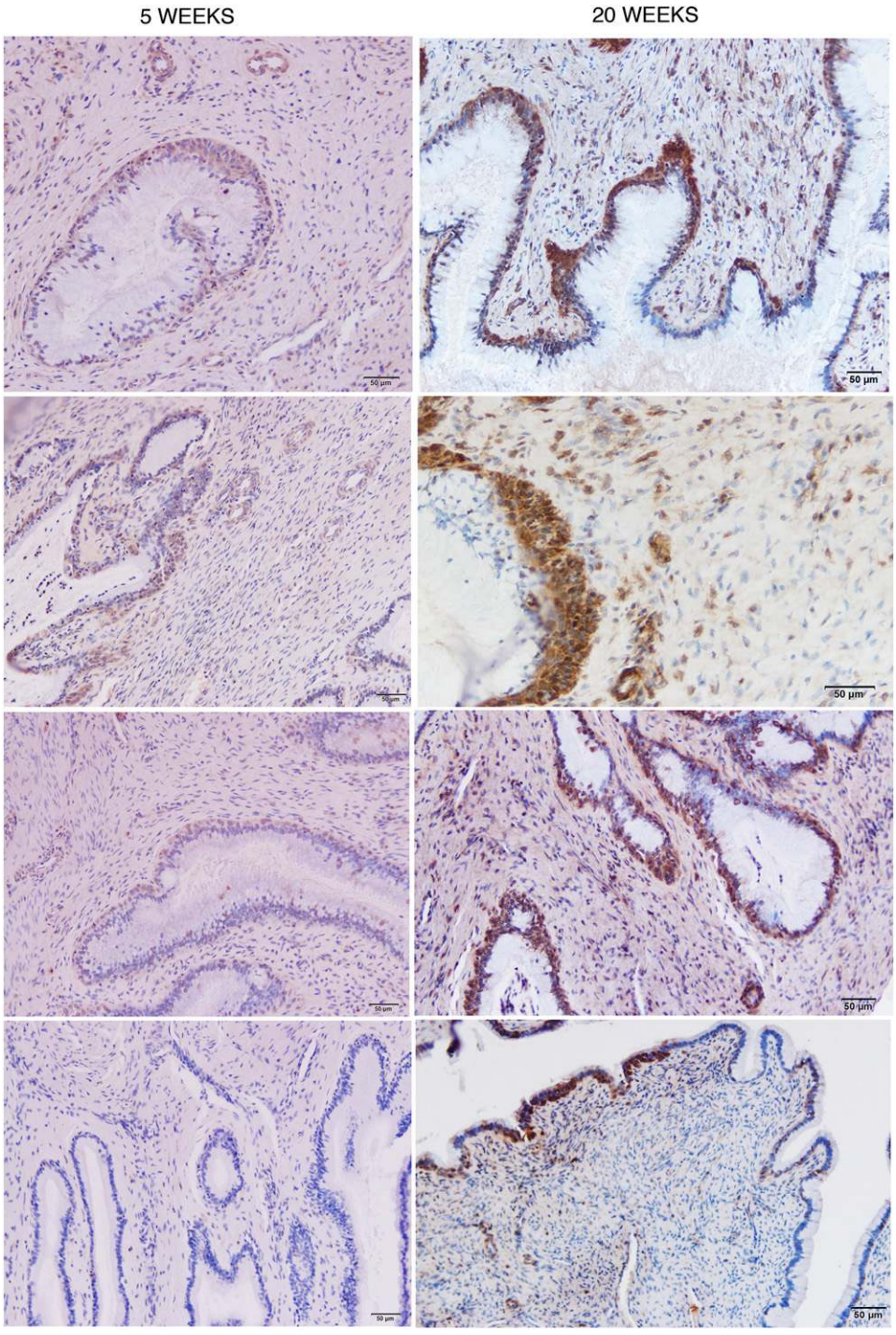

FIGURE 5. Increased staining of gp41t Ab^+ reserve cells at 20 wk compared with 5 wk. Each panel is from an individual animal. Scale bars, 50 μm.

Abs that increased from 5 to 20 wk as a correlate of the maturation of the protective effects of vaccination. Consistent with this hypothesis, we detected predominantly IgG Abs reactive with SIV oligomeric gp41 in WBs prior to WT SIV_{mac251} vaginal challenge that increased significantly ($p < 0.01$; 5-fold) between 5 and 20 wk in cervical tissues, vaginal tissues, and cervical vaginal tissues and fluids (CVF) (Fig. 2a, 2c, 2d). The gp160 and gp80 bands with which the Abs reacted most strongly in CVF and in serum (Fig. 2e) were shown, two decades ago, to be oligomeric complexes of gp41 (22–24). This conclusion was further supported by reactivity with rhesus mAbs to gp41, but not gp120 (25) (Fig. 2b) and, indeed, identical reactivity with oligomeric gp41 in WBs of mAb 4.9C and Abs in the FRT (red box, Fig. 2b). Cervical gp41-IgA Abs reacting mainly with oligomeric gp41 also increased between 5 and 20 wk in the cervical vaginal tissue extracts, CVF, and serum (data not shown). However, because IgA concentrations were 150–200-fold lower than IgG concentrations (Supplemental Table I), we subsequently focused on the role that IgG Abs might be playing in the temporal maturation of protection.

Cervical IgG Ab production and delivery

We initially stained sections to see whether IgG Abs might be detectable at the tissue sites where the inhibition of viral replication had been observed. We discovered, by this simple approach, that the numbers of IgG^+ cells in the cervix increased in the vaccinated animals compared with unvaccinated SIV^- controls and between 5 and 20 wk in the vaccinated animals (Fig. 3a, 3b; Supplemental

Downloaded from http://www.jimmunol.org/ by guest on August 4, 2022

Fig. 1a). The IgG$^+$ cells in the submucosa were identified as plasma cells by their morphology and by staining for a plasma cell marker, CD138 (26) (data not shown), whereas the IgG$^+$ cells just beneath the columnar epithelium lining the cervix were identified as epithelial reserve cells (27) by their epithelial morphology, location in the TZ and adjoining endocervix (Fig. 3b), and the colocalization of IgG staining with the reserve cell marker (28), cytokeratin 5 (CK5) (Fig. 3c, 3d).

The images of the location of IgG in the reserve epithelium struck us as somewhat similar to the images of FcRn in murine and human uterine and vaginal epithelium (29). Therefore, we hypothesized that the RM cervical reserve epithelium might express FcRn$^+$, and we tested this hypothesis by staining cervical sections with Ab to FcRn. We found that IgG and FcRn colocalized in CK5$^+$ cervical reserve epithelium (Fig. 3e–h). IgG$^+$-staining plasma cells increased ~2.5-fold and cervical reserve epithelium increased >10-fold between 5 and 20 wk (Fig. 3i).

Local trimeric gp41 Ab production and delivery

Thus, we had visualized a potentially generic system for local production and concentration of IgG Abs in the TZ of the cervix. To show that such a system concentrated gp41-specific IgG Abs at the portal of entry, we used reverse immunohistochemistry (RIHC) (30) to stain cells containing gp41 Abs. For RIHC staining, we generated a soluble trimeric gp41 (sgp41t) ectodomain recombinant protein, which was designed to mimic in vivo Ags, such as trimeric gp41 (gp41t) six-helical bundles ("stumps") left in the viral membrane following gp120 shedding (31). The sgp41t protein retained cluster I and II immunodominant epitopes (32, 33) but lacked the hydrophobic transmembrane domain, the membrane proximal external region, and fusion peptide regions of gp41 (Supplemental Fig. 2). With this reagent, we found that gp41t Abs were readily detectable in plasma cells and FcRn$^+$ cervical reserve cells (Fig. 4 a–d) in 4/4 animals at 20 wk but only faint staining was seen compared with naive controls (Fig. 4e, 4f) in four animals at 5 wk (Fig. 5). The increased staining of reserve epithelium at 20 wk compared with 5 wk is consistent with the increased gp41t$^+$ plasma cells in the submucosa, increased Abs to gp41t present in the tissues and CVF (Fig. 2), and maturation of protection.

Vaginal IgG Ab production and delivery

We next showed that there is a system in the vagina that locally produces and concentrates IgG Abs comparable to the one in the endocervix. In the vagina, IgG$^+$ cells beneath the epithelium increased in the vaccinated animals compared with unvaccinated SIV$^-$ controls (Supplemental Fig. 1b) between 5 and 20 wk (Fig. 6a, 6b). The IgG$^+$ cells were identified as plasma cells by their morphology and by staining with the plasma cell marker CD138 (Supplemental Fig. 3). In addition, ectopic tertiary lymphoid

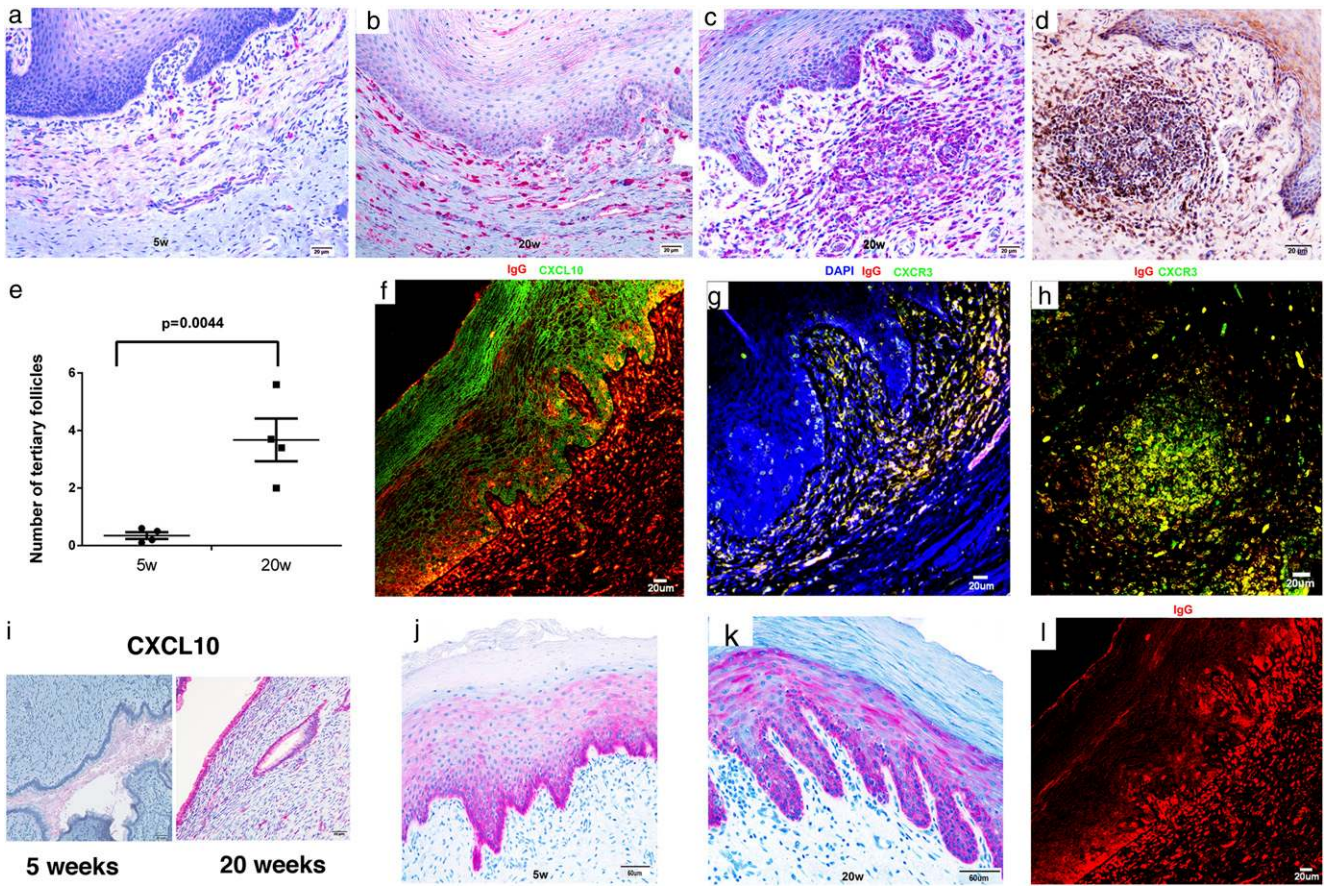

FIGURE 6. Recruitment of plasma cells to vagina and cervix, induction of ectopic lymphoid follicles, and localization of IgG in FcRn$^+$ basal epithelium in the lower FRT. Increased red-stained plasma cells in the submucosa at 5 wk (**a**) compared with 20 wk (**b**). (**c**–**e**) Increases in ectopic tertiary follicles in vagina between 5 and 20 wk. Follicles contain red-stained IgG$^+$ plasma cells (c) and brown-stained gp41t$^-$ Ab$^+$ cells (d). (**f**–**h**) Epithelial expression of CXCL10 and recruitment of CXCR3$^+$ plasma cells to the submucosa and ectopic follicles. In (f), CXCL10-expressing vaginal epithelium is stained green, and the IgG in plasma cells is stained red. The orange color in (f) is the result of IgG concentrated by the FcRn in CXCL10$^+$ basal epithelium (see also **j**–**l**). (g and h) CXCR3$^+$ IgG$^+$ plasma cells in the submucosa and in ectopic follicles are stained yellow. (**i**) Increased expression of CXCL10 between 5 and 20 wk in red-stained endocervical epithelium. (j and k) Mainly basal epithelial expression of FcRn at 5 and 20 wk. (l) IgG concentrated in the FcRn$^+$ epithelium above IgG$^+$ plasma cells. Image corresponds to (f) but only red-staining IgG is shown. Scale bars, 20 μm (a–d, f–h, i, l); 60 μm (j, k).

Downloaded from http://www.jimmunol.org/ by guest on August 4, 2022

follicles in the vagina, which contained IgG^+ and $gp41t^-$ Ab^+ plasma cells (Fig. 6c, 6d), increased in number by 9-fold between 5 and 20 wk (Fig. 6e). Because murine vaginal epithelial cells are a known source of chemokines that recruit CTLs to the FRT (34), we asked whether epithelium might be a source of chemokines to recruit plasma cells in RMs. We found that expression of CXCL10 at 20 wk in vaginal multilayered squamous epithelium (Fig. 6f) was associated with recruitment of $CXCR3^+$ plasma cells to vaginal submucosa and into follicles (Fig. 6g, 6h). Similarly, CXCL10 expression increased in endocervical epithelium between 5 and 20 wk as a mechanism to recruit plasma cells to that site (Fig. 6i).

FcRn also was constitutively expressed at approximately comparable levels at 5 and 20 wk postvaccination in the vagina and ectocervix. FcRn was expressed primarily in the basal layers of the multilayered squamous epithelium (Fig. 6j, 6k), in close proximity to the plasma cells and follicles producing IgG Abs. The concentration of IgG in basal epithelium above the IgG^+ cells in the submucosa at 20 wk postvaccination (Fig. 6l) is consistent with the proposed system in which spatial proximity between cells producing IgG Abs to FcRn-expressing epithelium could concentrate Abs to intercept virus that has traversed the mucosal barrier to that depth.

Potential protective mechanisms for gp41t Abs in the FRT

Thus, the gp41t Abs are located at the right time and right place to intercept virus at entry and immediately contain infection by a number of mechanisms. These include classical extracellular neutralization (35) and intracellular neutralization (36), in which virus captured by IgG bound to FcRn is diverted from the early endosome pathway and degraded in lysosomes, as well as virus binding and capture (37). We investigated neutralization in vitro in assays using unheated sera as a source of complement (17). The 20-wk sera neutralized TCLA SIV_{mac251} at a higher titer than did the 5-wk sera (Fig. 7a). However, activity against the somewhat more neutralization-resistant $SIV_{mac251\text{-}32H}$ strain or the challenge stock of SIV_{mac251} was weaker and did not differ significantly between 5 and 20 wk. We interpret reductions in viral infectivity of only 50% over a broad range of dilutions at 20 wk as plateau effects of a neutralization-resistant fraction of virus (Fig. 7b, 7c).

Virus capture and intracellular neutralization were assayed in $FcRn^+$ HEC-1-A cells in a Transwell system (19) to mimic, in vitro, these activities in cervical reserve and vaginal epithelium (Fig. 8a). We tested sera from a chronically infected animal as a positive control in this assay, as well as the rhesus mAb 4.9C, because of the similar reactivity of that Ab and anti-oligomeric gp41 Abs in WBs (Fig. 2b). IgG and FcRn colocalized in an early endosomal pathway in this assay system (Fig. 8b), as did IgG from the positive-control sera and SIV (Fig. 8c). A significantly greater fraction of the SIV captured by positive-control sera compared with sera from uninfected animals was diverted to $LAMP1^+$ lysosomes for degradation (Fig. 8d, 8g), as described for intracellular neutralization (36). Positive-control sera, 20-wk sera and cervical tissue extracts, and mAb 4.9C all significantly decreased transcytosis in this system, whereas sera from uninfected animals and 5 wk-sera and tissue extracts did not (Fig. 8e, 8f). We showed that the FcRn-translocation pathway was involved in capture and transcytosis by reversing these activities with SA binding of IgG, which acts as a competitive inhibitor of FcRn-mediated transport (Fig. 8e, 8f) (20, 21).

Discussion

As one of the interfaces with the external environment, the mucosa of the FRT has evolved multiple mechanisms to protect against pathogens. In this article, we describe a spatial and temporal correlate of the maturation of protection against high-dose vaginal challenge conferred by vaccination with an effective live attenuated vaccine.

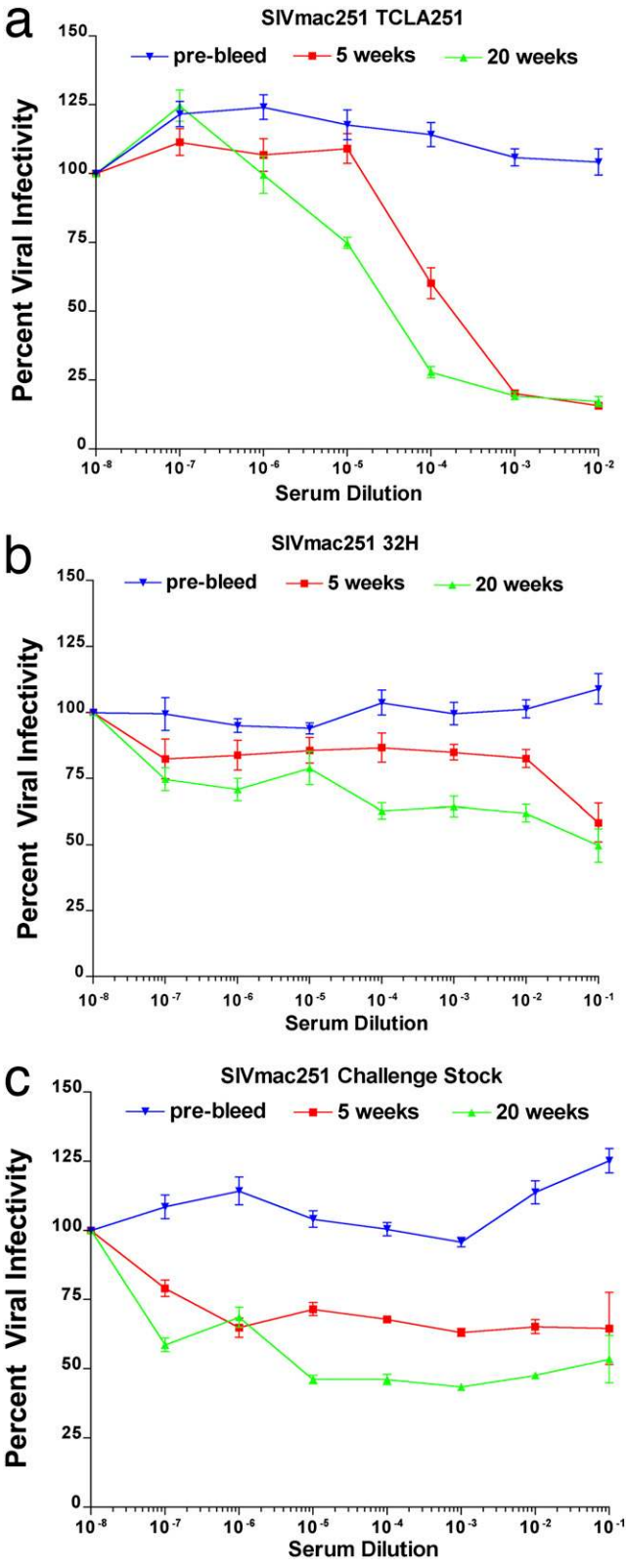

FIGURE 7. Extracellular neutralization. (**a**) Sera neutralize TCLA SIV_{mac251} at 20 wk at higher titer compared with at 5 wk. Compared with prebleed sera, $SIV_{mac251\text{-}32H}$ (**b**) and the challenge stock of WT SIV_{mac251} (**c**) are partially neutralized over a broad range of dilutions, to 50% reduction in infectivity with 20-wk sera.

We found that vaccination with SIVΔnef induced an organized system of local Ab production and concentration that correlated with reduction in VLs in the FRT tissues to undetectable or very low

Downloaded from http://www.jimmunol.org/ by guest on August 4, 2022

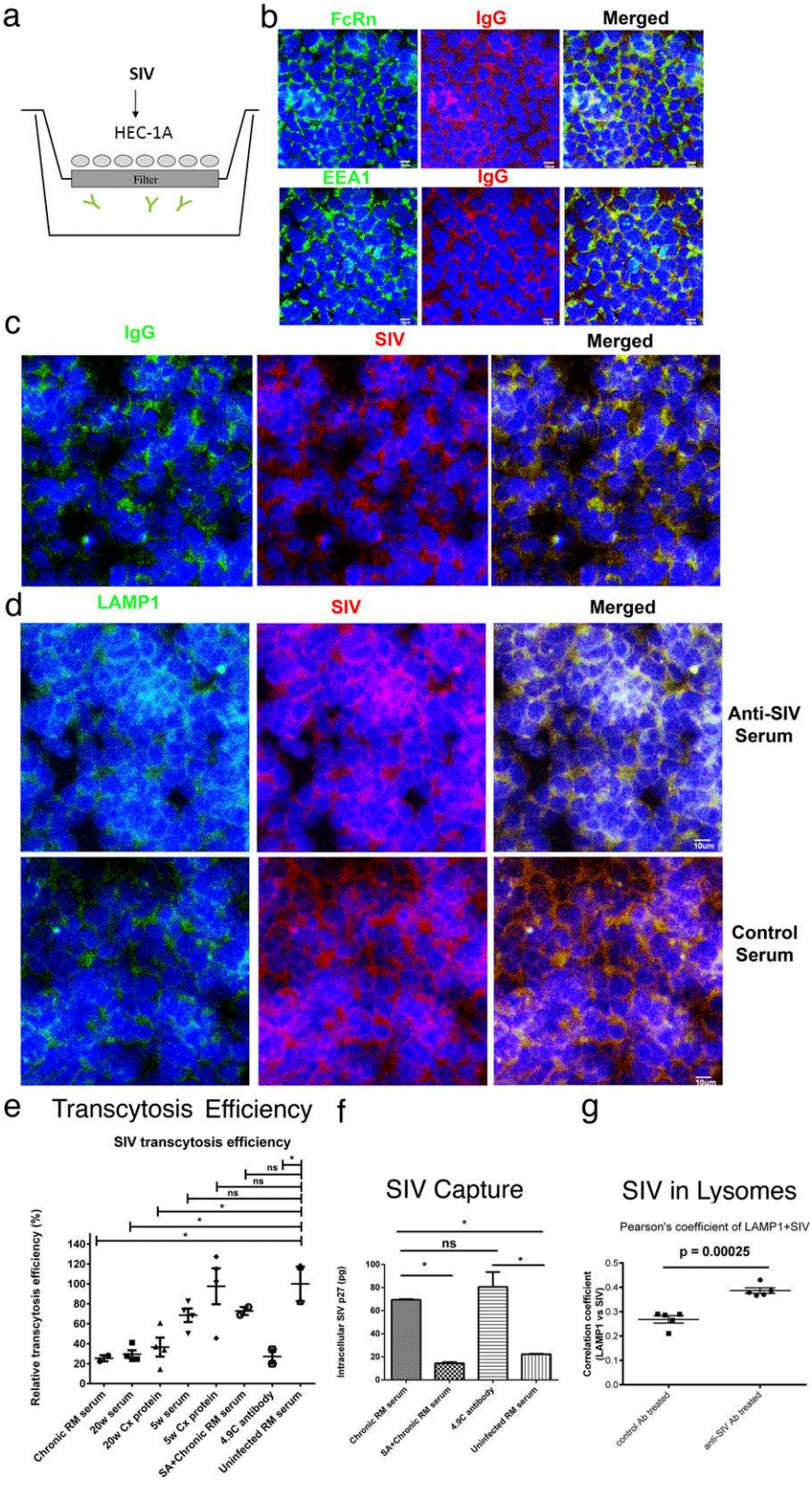

FIGURE 8. Transcytosis, virus capture, and intracellular neutralization (**a**) HEC-1-A-FcRn$^+$ epithelial cell line and Transwell system to assay SIV capture, transcytosis, and intracellular neutralization. SIV is added to the upper well. IgG Abs (depicted as Y) are in the lower well. (**b**) IgG and the FcRn colocalize in the EEA1$^+$ early endosomal pathway. (**c** and **d**) SIV is captured in the FcRn transcytosis pathway and diverted to LAMP1$^+$ lysosomes by anti-SIV sera but not control sera. Scale bars, 10 μm. (**e** and **f**) Quantification. Transcytosis of SIV in the Transwell system is significantly decreased by Abs from an SIV-infected RM. Sera and a cervical tissue extract (Cx Protein) from an animal at 20 wk post-vaccination and the rhesus mAb 4.9C, which reacts identically in WBs to the cervical tissue Abs to oligomeric gp41. Sera and cervical tissue extract (Cx protein) at 5 wk postvaccination and sera from uninfected RMs do not significantly decrease transcytosis. The FcRn-translocation pathway was required for capture and transcytosis, because SA, which blocks the interaction between FcRn and IgG (20, 21), diminished viral capture and the inhibitory effect on viral transcytosis by SIV-infected RM serum. (**g**) Colocalization of SIV with LAMP1$^+$ lysosomes in HEC-1-A cells treated with anti-SIV serum but not with control serum from an uninfected animal. Extent of colocalization is expressed as Pearson correlation coefficients. The small p values reflect the small group SD relative to the magnitude of the difference between groups. ns, not significant.

levels in vaccinated animals compared with unvaccinated animals. In the cervix, local production of gp41t IgG Abs by plasma cells underlying FcRn$^+$ cervical reserve epithelium acts as a system to deliver and concentrate these Abs at a critical site and time where establishment and expansion of infected founder populations precede production of sufficient virus and infected cells to disseminate and rapidly establish a robust systemic infection (1, 10–12). In the vagina, Ab production and delivery by plasma cells and ectopic follicles underlying FcRn$^+$ basal epithelium would similarly concentrate gp41t Abs as a second line of defenses to prevent viruses traversing the multilayered squamous epithelial barrier from infecting target cells in the underlying submucosa.

There are four important components of this Ab correlate of local protection induced by SIVΔnef vaccination (Fig. 9): recruitment of

Downloaded from http://www.jimmunol.org/ by guest on August 4, 2022

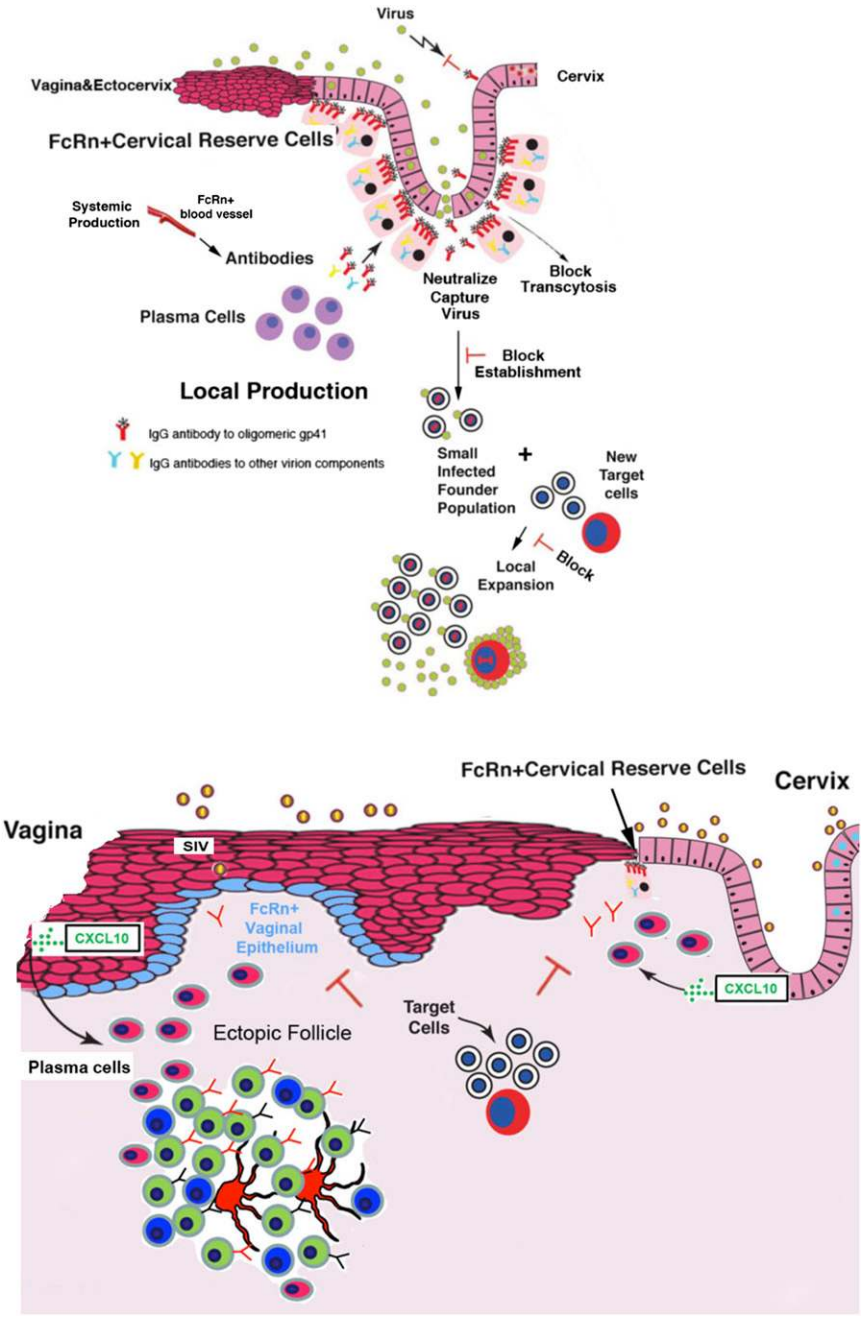

FIGURE 9. Model of local production and FcRn-mediated delivery of Abs and effects of anti-gp41t Abs at the cervical (*upper panel*) and vaginal (*lower panel*) mucosal borders. In the TZ and endocervix, IgG Abs to gp41t are produced by plasma cells. These Abs are collected efficiently because of their spatial proximity to $FcRn^+$ cervical reserve epithelium and, thereby, are concentrated on the path of virus entry. The concentrated Abs can interfere by several potential mechanisms, with the establishment and expansion of infected founder populations. In both the vagina and cervix, mucosal epithelial expression of CXCL10 recruits $CXCR3^+$ plasma cells. In the vagina, ectopic follicles are induced, and Abs are produced by plasma cells in the submucosa and follicles. FcRn expression in the basal epithelium concentrates these IgG Abs on the path of virus that has traversed the multilayer epithelium lining the vagina and ectocervix to prevent infection of target cells in the submucosa.

plasma cells and formation of ectopic follicles; local production of gp41t Abs; FcRn-mediated mechanisms in cervical reserve and basal vaginal epithelium concentrate SIV-specific IgG Ab to intercept virus on entry and inhibit the necessary interactions with target cells to establish infection at the portal of entry; and an active role for the mucosal epithelium lining the cervix and vagina in recruiting plasma cells and increasing ectopic follicles, as well as concentrating Abs by FcRn-mediated mechanisms.

One critical feature of this system is locating a production source in close proximity to the delivery system. In principle, this feature overcomes diffusion constraints for Abs coming from the circulation to achieve the high local concentration of Abs to intercept virus at entry by mass action mechanisms we next describe. We also note in this study that direct visualization of gp41t staining of reserve epithelium is consistent with the idea that we can see IgG Abs in the cells because the high local concentrations exceed the normal FcRn flux rate for IgG of multiple specificities.

Ab production and concentration in the FRT could likely protect through multiple cooperative, complementary, and nonexclusive mechanisms. We think that the most important of these mechanisms is an example of the general principle of concentration-dependent protection at mucosal frontlines. This concept provides a theoretical framework to understand the increased efficacy of protection against acquisition by passive immunization with more potent, new-generation mAbs against HIV (38), as well as the importance of the FcRn in protecting mice against HSV-2 infection (29). For SIVΔnef, we think that this principle applies through the cooperative "mass action" effects of the high local concentrations of reactants—Ab and virus—in the small volume where they would first interact at the portal of entry. These concentration-dependent effects might amplify in vivo what appear, from in vitro assays, to be relatively weak extracellular neutralization, and they might similarly amplify protective mechanisms related to virus binding and trapping to prevent access to susceptible target cells (39).

Downloaded from http://www.jimmunol.org/ by guest on August 4, 2022

What are the similarities and differences between this system of local Ab production and concentration as a correlate of SIVΔnef's robust protection and other potential mechanisms of protection? First, vaginal IgG Abs with neutralizing or Ab-dependent cell-mediated cytotoxicity (ADCC) activity were shown to protect against vaginal simian HIV challenge (40). However, these Abs were elicited by immunization with a gp41t–peptide from which the immunodominant cluster I epitope had been deleted. In contrast, IgG Abs to gp41t elicited by SIVΔnef are more reminiscent of the HIV-1 mAb F240 (35), which strongly binds to the cluster 1 epitope. Moreover, ADCC activity and NK cell and macrophage numbers as ADCC effectors in cervical vaginal tissues do not correlate with the maturation of SIVΔnef protection (M. Alpert, D. Evans, et al. unpublished observations; 41). Second, the FcRn pathway has been used to enhance Ag presentation and the B and T cell responses in the mouse to HIV-Gag, as well as deliver passively transferred Abs that increased protection against HSV-2 infection (29, 42, 43). However, there is no evidence that these strategies reproduced the SIVΔnef system of local Ab production and concentration. Lastly, a new chemokine "pull" strategy for recruiting T cells to the genital tract was shown to enhance local protection against HSV-2 in mice (44). In contrast, we do not find an increase in SIV-specific CD8 T cells in the FRT as a correlate of the maturation of protection with SIVΔnef vaccination (45).

The robust protection afforded by live attenuated SIV vaccines (4–7) provides motive and rationale to identify correlates of that protection to guide development of HIV-1 vaccine candidates that would circumvent the safety issues (46, 47) associated with SIVΔnef vaccination. Thus, reproducing the system described in this study of local Ab production and concentration at mucosal frontlines is a promising design principle to incorporate into the development and assessment of vaccines to prevent HIV-1 transmission to women.

Acknowledgments

We thank R. Desrosiers and C. Miller for virus stocks; C. Miller for tissue samples from uninfected animals and from unvaccinated and infected animals; A. Carville for expert veterinary care; E. Curran and A. Miller for assistance with tissue processing and analysis; J. Estes, E. Hunter, A. Iwasaki, D. Montefiori, J. Moore, G. Spear, C. Wira, and S. Zolla-Pazner for helpful discussions; and C. O'Neill and T. Leonard for help in preparing the manuscripts and figures. The AIDS Research and Reference Reagent Program, Division of AIDS, National Institute of Allergy and Infectious Diseases, National Institutes of Health provided $SIV_{mac251\ 32H}$ from Drs. M. Cranage and R. Desrosiers and SIV_{mac251} antiserum from Drs. K. Reimann and D. Montefiori.

Disclosures

D.W. is an employee of Zeptometrix, and S.M. is an employee of ImmPheron Inc.

References

1. Haase, A. T. 2010. Targeting early infection to prevent HIV-1 mucosal transmission. *Nature* 464: 217–223.
2. Quinn, T. C., and J. Overbaugh. 2005. HIV/AIDS in women: an expanding epidemic. *Science* 308: 1582–1583.
3. Daniel, M. D., F. Kirchhoff, S. C. Czajak, P. K. Sehgal, and R. C. Desrosiers. 1992. Protective effects of a live attenuated SIV vaccine with a deletion in the *nef* gene. *Science* 258: 1938–1941.
4. Johnson, R. P. 1999. Live attenuated AIDS vaccines: hazards and hopes. *Nat. Med.* 5: 154–155.
5. Koff, W. C., P. R. Johnson, D. I. Watkins, D. R. Burton, J. D. Lifson, K. J. Hasenkrug, A. B. McDermott, A. Schultz, T. J. Zamb, R. Boyle, and R. C. Desrosiers. 2006. HIV vaccine design: insights from live attenuated SIV vaccines. *Nat. Immunol.* 7: 19–23.
6. Reynolds, M. R., A. M. Weiler, K. L. Weisgrau, S. M. Piaskowski, J. R. Furlott, J. T. Weinfurter, M. Kaizu, T. Soma, E. J. León, C. MacNair, et al. 2008. Macaques vaccinated with live-attenuated SIV control replication of heterologous virus. *J. Exp. Med.* 205: 2537–2550.
7. Reynolds, M. R., A. M. Weiler, S. M. Piaskowski, H. L. Kolar, A. J. Hessell, M. Weiker, K. L. Weisgrau, E. J. León, W. E. Rogers, R. Makowsky, et al. 2010. Macaques vaccinated with simian immunodeficiency virus SIVmac239Δ nef delay acquisition and control replication after repeated low-dose heterologous SIV challenge. *J. Virol.* 84: 9190–9199.
8. Connor, R. I., D. C. Montefiori, J. M. Binley, J. P. Moore, S. Bonhoeffer, A. Gettie, E. A. Fenamore, K. E. Sheridan, D. D. Ho, P. J. Dailey, and P. A. Marx. 1998. Temporal analyses of virus replication, immune responses, and efficacy in rhesus macaques immunized with a live, attenuated simian immunodeficiency virus vaccine. *J. Virol.* 72: 7501–7509.
9. Roopenian, D. C., and S. Akilesh. 2007. FcRn: the neonatal Fc receptor comes of age. *Nat. Rev. Immunol.* 7: 715–725.
10. Miller, C. J., Q. Li, K. Abel, E.-Y. Kim, Z.-M. Ma, S. Wietgrefe, L. La Franco-Scheuch, L. Compton, L. Duan, M. D. Shore, et al. 2005. Propagation and dissemination of infection after vaginal transmission of simian immunodeficiency virus. [Published erratum appears in 2005 *J. Virol.* 79: 11552.] *J. Virol.* 79: 9217–9227.
11. Li, Q., J. D. Estes, P. M. Schlievert, L. Duan, A. J. Brosnahan, P. J. Southern, C. S. Reilly, M. L. Peterson, N. Schultz-Darken, K. G. Brunner, et al. 2009. Glycerol monolaurate prevents mucosal SIV transmission. *Nature* 458: 1034–1038.
12. Zhang, Z. Q., T. Schuler, M. Zupancic, S. Wietgrefe, K. A. Reimann, T. A. Reinhart, M. Rogan, W. Cavert, C. J. Miller, R. S. Veazey, et al. 1999. Sexual transmission and propagation of SIV and HIV in resting and activated $CD4^+$ T cells. *Science* 286: 1353–1357.
13. Zeng, M., A. J. Smith, S. W. Wietgrefe, P. J. Southern, T. W. Schacker, C. S. Reilly, J. D. Estes, G. F. Burton, G. Silvestri, J. D. Lifson, et al. 2011. Cumulative mechanisms of lymphoid tissue fibrosis and T cell depletion in HIV-1 and SIV infections. *J. Clin. Invest.* 121: 998–1008.
14. Salisch, N. C., D. E. Kaufmann, A. S. Awad, R. K. Reeves, D. P. Tighe, Y. Li, M. Piatak, Jr., J. D. Lifson, D. T. Evans, F. Pereyra, et al. 2010. Inhibitory TCR coreceptor PD-1 is a sensitive indicator of low-level replication of SIV and HIV-1. *J. Immunol.* 184: 476–487.
15. Kozlowski, P. A., R. M. Lynch, R. R. Patterson, S. Cu-Uvin, T. P. Flanigan, and M. R. Neutra. 2000. Modified wick method using Weck-Cel sponges for collection of human rectal secretions and analysis of mucosal HIV antibody. *J. Acquir. Immune Defic. Syndr.* 24: 297–309.
16. Caffrey, M., M. Cai, J. Kaufman, S. J. Stahl, P. T. Wingfield, D. G. Covell, A. M. Gronenborn, and G. M. Clore. 1998. Three-dimensional solution structure of the 44 kDa ectodomain of SIV gp41. *EMBO J.* 17: 4572–4584.
17. Freissmuth, D., A. Hiltgartner, C. Stahl-Hennig, D. Fuchs, K. Tenner-Racz, P. Racz, K. Uberla, A. Strasak, M. P. Dierich, H. Stoiber, and B. Falkensammer. 2010. Analysis of humoral immune responses in rhesus macaques vaccinated with attenuated SIVmac239Deltanef and challenged with pathogenic SIVmac251. *J. Med. Primatol.* 39: 97–111.
18. Means, R. E., T. Greenough, and R. C. Desrosiers. 1997. Neutralization sensitivity of cell culture-passaged simian immunodeficiency virus. *J. Virol.* 71: 7895–7902.
19. Shen, R., E. R. Drelichman, D. Bimczok, C. Ochsenbauer, J. C. Kappes, J. A. Cannon, D. Tudor, M. Bomsel, L. E. Smythies, and P. D. Smith. 2010. GP41-specific antibody blocks cell-free HIV type 1 transcytosis through human rectal mucosa and model colonic epithelium. *J. Immunol.* 184: 3648–3655.
20. Antohe, F., L. Rădulescu, A. Gafencu, V. Gheţie, and M. Simionescu. 2001. Expression of functionally active FcRn and the differentiated bidirectional transport of IgG in human placental endothelial cells. *Hum. Immunol.* 62: 93–105.
21. Maidji, E., S. McDonagh, O. Genbacev, T. Tabata, and L. Pereira. 2006. Maternal antibodies enhance or prevent cytomegalovirus infection in the placenta by neonatal Fc receptor-mediated transcytosis. *Am. J. Pathol.* 168: 1210–1226.
22. Pinter, A., W. J. Honnen, S. A. Tilley, C. Bona, H. Zaghouani, M. K. Gorny, and S. Zolla-Pazner. 1989. Oligomeric structure of gp41, the transmembrane protein of human immunodeficiency virus type 1. *J. Virol.* 63: 2674–2679.
23. Zolla-Pazner, S., M. K. Gorny, W. J. Honnen, and A. Pinter. 1989. Reinterpretation of human immunodeficiency virus western blot patterns. *N. Engl. J. Med.* 320: 1280–1281.
24. Parekh, B. S., C. P. Pau, T. C. Granade, M. Rayfield, K. M. De Cock, H. Gayle, G. Schochetman, and J. R. George. 1991. Oligomeric nature of transmembrane glycoproteins of HIV-2: procedures for their efficient dissociation and preparation of Western blots for diagnosis. *AIDS* 5: 1009–1013.
25. Cole, K. S., M. Alvarez, D. H. Elliott, H. Lam, E. Martin, T. Chau, K. Micken, J. L. Rowles, J. E. Clements, M. Murphey-Corb, et al. 2001. Characterization of neutralization epitopes of simian immunodeficiency virus (SIV) recognized by rhesus monoclonal antibodies derived from monkeys infected with an attenuated SIV strain. *Virology* 290: 59–73.
26. Sanderson, R. D., P. Lalor, and M. Bernfield. 1989. B lymphocytes express and lose syndecan at specific stages of differentiation. *Cell Regul.* 1: 27–35.
27. Smedts, F., F. Ramaekers, S. Troyanovsky, M. Pruszczynski, H. Robben, B. Lane, I. Leigh, F. Plantema, and P. Vooijs. 1992. Basal-cell keratins in cervical reserve cells and a comparison to their expression in cervical intraepithelial neoplasia. *Am. J. Pathol.* 140: 601–612.
28. Martens, J. E., F. M. Smedts, D. Ploeger, T. J. Helmerhorst, F. C. Ramaekers, J. W. Arends, and A. H. Hopman. 2009. Distribution pattern and marker profile show two subpopulations of reserve cells in the endocervical canal. *Int. J. Gynecol. Pathol.* 28: 381–388.

Downloaded from http://www.jimmunol.org/ by guest on August 4, 2022

29. Li, Z., S. Palaniyandi, R. Zeng, W. Tuo, D. C. Roopenian, and X. Zhu. 2011. Transfer of IgG in the female genital tract by MHC class I-related neonatal Fc receptor (FcRn) confers protective immunity to vaginal infection. *Proc. Natl. Acad. Sci. USA* 108: 4388–4393.
30. Tsuge, S., Y. Mizutani, K. Matsuoka, T. Sawasaki, Y. Endo, K. Naruishi, H. Maeda, S. Takashiba, K. Shiogama, K. Inada, and Y. Tsutsumi. 2011. Specific in situ visualization of plasma cells producing antibodies against *Porphyromonas gingivalis* in gingival radicular cyst: application of the enzyme-labeled antigen method. *J. Histochem. Cytochem.* 59: 673–689.
31. Moore, P. L., E. T. Crooks, L. Porter, P. Zhu, C. S. Cayanan, H. Grise, P. Corcoran, M. B. Zwick, M. Franti, L. Morris, et al. 2006. Nature of nonfunctional envelope proteins on the surface of human immunodeficiency virus type 1. *J. Virol.* 80: 2515–2528.
32. Zolla-Pazner, S. 2004. Identifying epitopes of HIV-1 that induce protective antibodies. *Nat. Rev. Immunol.* 4: 199–210.
33. Xu, J.-Y., M. K. Gorny, T. Palker, S. Karwaska, and S. Zolla-Pazner. 1991. Epitope mapping of two immunodominant domains of gp41, the transmembrane protein of HIV-1. Using ten human monoclonal antibodies. *J. Virol.* 65: 4832–4838.
34. Nakanishi, Y., B. Lu, C. Gerard, and A. Iwasaki. 2009. CD8(+) T lymphocyte mobilization to virus-infected tissue requires CD4(+) T-cell help. *Nature* 462: 510–513.
35. Burton, D. R., A. J. Hessell, B. F. Keele, P. J. Klasse, T. A. Ketas, B. Moldt, D. C. Dunlop, P. Poignard, L. A. Doyle, L. Cavacini, et al. 2011. Limited or no protection by weakly or nonneutralizing antibodies against vaginal SHIV challenge of macaques compared with a strongly neutralizing antibody. *Proc. Natl. Acad. Sci. USA* 108: 11181–11186.
36. Bai, Y., L. Ye, D. B. Tesar, H. Song, D. Zhao, P. J. Björkman, D. C. Roopenian, and X. Zhu. 2011. Intracellular neutralization of viral infection in polarized epithelial cells by neonatal Fc receptor (FcRn)-mediated IgG transport. *Proc. Natl. Acad. Sci. USA* 108: 18406–18411.
37. Burrer, R., S. Haessig-Einius, A.-M. Aubertin, and C. Moog. 2005. Neutralizing as well as non-neutralizing polyclonal immunoglobulin (Ig)G from infected patients capture HIV-1 via antibodies directed against the principal immunodominant domain of gp41. *Virology* 333: 102–113.
38. Shingai, M., Y. Nishimura, F. Klein, H. Mouquet, O. K. Donau, R. Plishka, A. Buckler-White, M. Seaman, M. Piatak, Jr., J. D. Lifson, et al. 2013. Antibody-mediated immunotherapy of macaques chronically infected with SHIV suppresses viraemia. *Nature* 503: 277–280.
39. Hope, T. J. 2011. Moving ahead an HIV vaccine: to neutralize or not, a key HIV vaccine question. *Nat. Med.* 17: 1195–1197.
40. Bomsel, M., D. Tudor, A. S. Drillet, A. Alfsen, Y. Ganor, M. G. Roger, N. Mouz, M. Amacker, A. Chalifour, L. Diomede, et al. 2011. Immunization with HIV-1 gp41 subunit virosomes induces mucosal antibodies protecting nonhuman primates against vaginal SHIV challenges. *Immunity* 34: 269–280.
41. Shang, L., A. J. Smith, L. Duan, K. E. Perkey, L. Qu, S. Wietgrefe, M. Zupancic, P. J. Southern, K. Masek-Hammerman, R. K. Reeves, et al. 2014. NK cell responses to SIV vaginal exposure in naive and vaccinated rhesus macaques. *J. Immunol.* 193: 277–284.
42. Ye, L., R. Zeng, Y. Bai, D. C. Roopenian, and X. Zhu. 2011. Efficient mucosal vaccination mediated by the neonatal Fc receptor. *Nat. Biotechnol.* 29: 158–163.
43. Lu, L., S. Palaniyandi, R. Zeng, Y. Bai, X. Liu, Y. Wang, C. D. Pauza, D. C. Roopenian, and X. Zhu. 2011. A neonatal Fc receptor-targeted mucosal vaccine strategy effectively induces HIV-1 antigen-specific immunity to genital infection. *J. Virol.* 85: 10542–10553.
44. Shin, H., and A. Iwasaki. 2012. A vaccine strategy that protects against genital herpes by establishing local memory T cells. *Nature* 491: 463–467.
45. Sasikala-Appukuttan, A. K., H. O. Kim, N. J. Kinzel, J. J. Hong, A. J. Smith, R. Wagstaff, C. Reilly, M. Piatak, Jr., J. D. Lifson, R. K. Reeves, et al. 2013. Location and dynamics of the immunodominant CD8 T cell response to SIVΔnef immunization and SIVmac251 vaginal challenge. PLoS ONE.
46. Baba, T. W., Y. S. Jeong, D. Pennick, R. Bronson, M. F. Greene, and R. M. Ruprecht. 1995. Pathogenicity of live, attenuated SIV after mucosal infection of neonatal macaques. *Science* 267: 1820–1825.
47. Baba, T. W., V. Liska, A. H. Khimani, N. B. Ray, P. J. Dailey, D. Penninck, R. Bronson, M. F. Greene, H. M. McClure, L. N. Martin, and R. M. Ruprecht. 1999. Live attenuated, multiply deleted simian immunodeficiency virus causes AIDS in infant and adult macaques. *Nat. Med.* 5: 194–203.